JOURNAL OF MATERIALS SCIENCE 26 (1991) 3057–3061

Cation interdiffusion between thick film of $YBa_2Cu_3O_{7-\delta}$ and ceramic substrate

X. M. LI, Y. T. CHOU
Department of Materials Science and Engineering and Materials Research Center, Lehigh University, Bethlehem, PA 18015, USA
Y. H. HU, C. L. BOOTH
E. I. Du Pont de Nemours and Company, Experimental Station, Wilmington, DE 19880, USA

Thick films of superconducting oxides, $YBa_2Cu_3O_{7-\delta}$, were successfully made by conventional screen-printing technology on Al_2O_3, MgO, and ZrO_2 substrates. Interdiffusion between the superconductive film and substrate was investigated using analytical electron microscopy. The results indicate that MgO and ZrO_2 are superior to Al_2O_3 for substrate materials.

1. Introduction

Since the recent discovery of high-temperature oxide superconductors, $YBa_2Cu_3O_{7-\delta}$, extensive research has been conducted to improve their critical current density [1–8]. A number of studies have been also undertaken on mechanical forming processes such as hydrostatic extrusion [9, 10], wire drawing [9–11] and tape casting [12–15]. In electronic device applications, however, where screen printing is the most economical process for patterning devices, only limited attention has been paid to applying this technology to the new oxides [16–19].

A major concern in screen printing is the bonding between the film and the substrate which results from the chemical interdiffusion of cations across the film–substrate boundary during high temperature sintering. The interdiffusion, if excessive, can cause the formation of undesired compounds near the interface [20, 21]. Such reactions could diminish or even destroy the film's superconducting properties. The purpose of the present research is to obtain quantitative information about the interdiffusion of cations across the film–substrate boundary. Three substrate materials, single crystal MgO, polycrystalline Al_2O_3, and yttrium-stabilized ZrO_2, were used. The results of Al_2O_3 substrate were reported earlier [22], but are included here for the sake of comparison.

2. Experimental procedure

Three groups of specimens with different substrates were prepared in the study. The thick-film paste was made of $YBa_2Cu_3O_{7-\delta}$ powder with organic vehicles (surfactant, binder, and solvent), using three stages of roll milling for homogeneity. The thick-film patterns were screen printed on the substrates, dried at 120 °C for 20 min, and subsequently heat treated at 500 °C for organic burnout. The diffusion couples were sintered at four different temperatures under flowing oxygen: 900 °C for 5 h, 930 °C for 2 h, 950 °C for 1 h, and 1000 °C for 10 min. All couples were furnace-cooled to 450 °C, annealed for 6 h at 450 °C, and slowly cooled to room temperature. A superconductive film of 20 to 50 μm thickness was successfully printed on each substrate by the above thermal processing [19].

The resistance of the sintered specimens was determined with a standard d.c. four-point probe at a current of 0.5 mA. The best electrical results were obtained on couples with MgO and ZrO_2 substrates. Fig. 1 depicts the temperature dependence of resistance of a thick film on MgO substrate. The onset temperature (T_c) of superconductivity of this film is about 87 K and the superconducting transition is completed ($R = 0$) at 79 K. The X-ray diffraction patterns show that, except for some characteristic peaks of the substrate, the major peaks can be assigned to the orthorhombic superconducting phase (Fig. 2). Films printed on Al_2O_3 substrate showed a drop in resistance at about 80 K, but the resistance never reached a "zero" state. This weak superconducting behaviour is consistent with the diffusion results as discussed below.

The short diffusion path, meant that concentration profiles were measured with a Philips 400 T analytical electron microscope in the STEM mode, which has high precision in point measurement. In preparing a STEM specimen for the interdiffusion study, the specimen must contain a well defined interface. Small sections containing the interface were cut out from the sintered plate with a diamond saw. Two pieces of the sections were glued together with the superconductive phase facing each other and then mounted with epoxy in a silver tube of 2.5 mm opening and 3 mm outer diameter. The filled silver tube again was cut into discs with the interface situated perpendicular to the surface of the disc. By lapping and finish-polishing both sides of the disc, the disc thickness was reduced to about 50 μm. One side of the polished disc then was dimpled by a 15 mm brass wheel with 3 μm diamond paste and polished by a polishing wheel with 0.25 μm diamond paste. The dimpling step was carried out at several spots along the line perpendicular to the interface.

0022–2461/91 $03.00 + .12

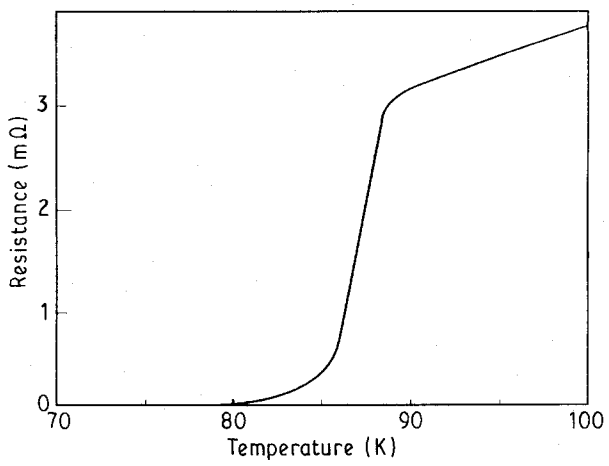

Figure 1 Temperature dependence of resistance of an $YBa_2Cu_3O_{7-\delta}$ thick film on MgO substrate. Specimen sintered at 950 °C for 1 h.

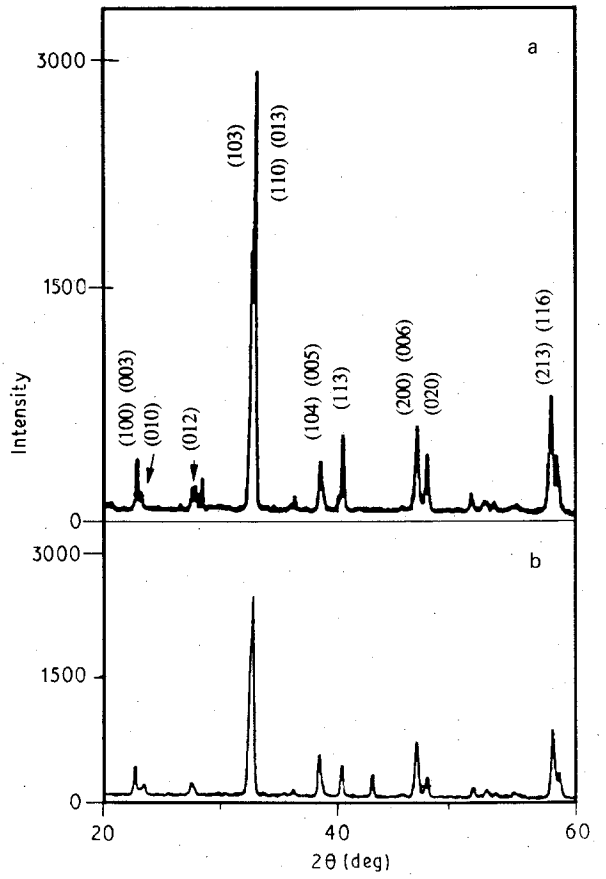

Figure 2 XRD pattern of an $YBa_2Cu_3O_{7-\delta}$ film on MgO substrate. Specimen sintered at 950 °C for 1 h (a) pure YBaCuO superconductor, (b) YBaCuO–MgO.

This procedure produced a homogeneous thin band 5 μm in thickness, about 20 μm in width and 150 μm in length. This band then was ion-milled using a Gatan unit at a 12° ion-beam incident angle on the cold stage at liquid nitrogen temperature and at 4 kV accelerated voltage and 0.5 A current. The ion-milled thin area was thinned further using a precise ion milling system (PIMS). The difference in hardness of the superconducting film and substrate materials means that a minor adjustment had to be made in the thickness of the dimpled band.

The characteristic X-ray spectra for all elements along the line perpendicular to the interface were determined by an analytical electron microscope at 120 keV. A quantitative analysis of the concentrations of cations was conducted based on the comparison with standard spectra of pure elements. The spectrum collection range was up to 20 keV. K lines were used for the quantitative analysis of all the elements except for Ba, for which the L lines were chosen because of its high atomic number.

3. Results and Discussion

For solid-state diffusion in a multiple-component system, the mass transfer of an individual species depends not only on its own chemical potential gradient, but also on gradient fields of other species present [22, 23]. A formal mathematical analysis for such a system, however, is highly complex and no such attempt is made in this study. Our approach is to present the measured data to illustrate the diffusion characteristics of cations for different substrate materials and correlate with the electrical measurements. By comparison, a suitable substrate for the film-substrate superconductors can be chosen.

3.1. Specimens with MgO substrates

Typical concentration profiles for specimens with MgO substrate are shown in Fig. 3a. The diffusion paths appear reasonably normal* except for Cu ions where a slight uphill diffusion is observed [22]. Change of sintering temperatures did not have a large effect on the shapes of cation distributions or on the characteristics of the diffusion paths, but it affected the penetration depths of each cation. The penetration depth of Mg^{2+} in the superconductive film was 5 to 10 μm for specimens sintered at 950 °C. For specimens sintered at 1000 °C, however, the depth was 25 to 30 μm. In the substrate, the penetration distances of Y^{3+}, Ba^{2+}, and Cu^{2+} were 20 to 25 μm for the 950 °C specimens and more than 40 μm for the 1000 °C specimens. In the latter case, the distance was beyond the measuring range of the instrument. For specimens sintered at 900 °C, it was difficult to prepare good specimens for AEM because of the weak interface bonding. For specimens sintered at 930 °C the measurement became difficult because a large number of pores were formed at the interface and within the film. Some of the 930 °C data were obtained from the bonded portions of the specimens which had very short diffusion paths for all cations: 1 to 2 μm for Mg^{2+} and approximately 5 μm for Y^{3+}, Ba^{2+}, and Cu^{2+}.

For specimens sintered at 950 °C, the weight fractions of Y^{3+}, Ba^{2+}, and Cu^{2+} measured at about 15 μm from the interface were 16, 49, and 34, respectively, while the concentration of Mg^{2+} was undetectable. The ratio of concentrations is consistent with the nominal ratio of the stoichiometric $YBa_2Cu_3O_{7-\delta}$ compound. For specimens sintered at 1000 °C, the

* By normal, we mean that the diffusion path behaves as in a conventional binary system.

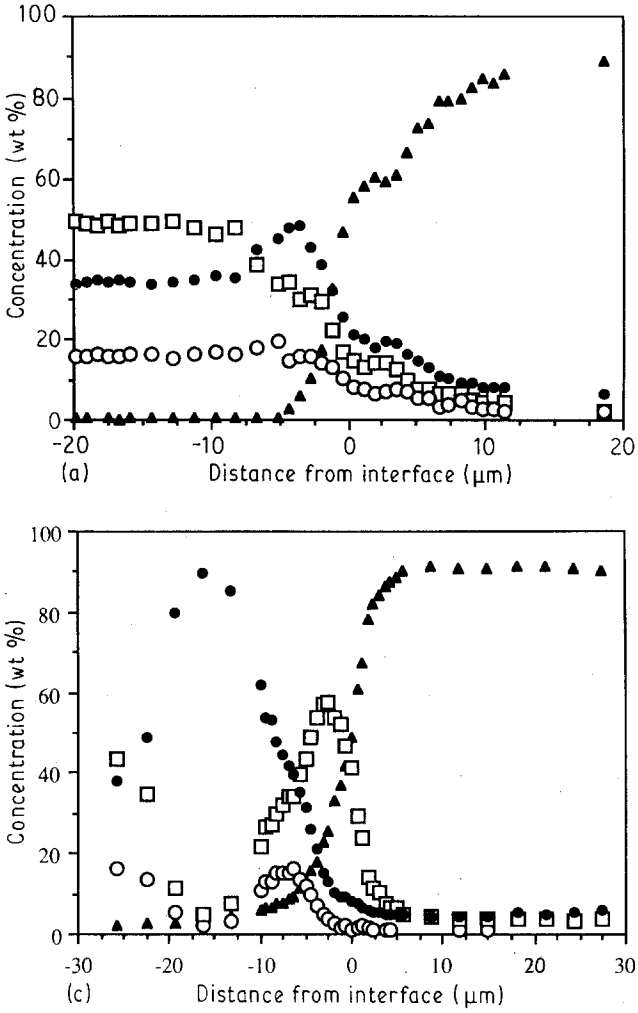

Figure 3 Concentration profiles of cations in screen-printed specimens of $YBa_2Cu_3O_{7-\delta}$ on three different substrates. (a) MgO, (b) ZrO_2, and (c) Al_2O_3. All specimens sintered at 950 °C for 1 h. The interface is located at $x = 0$ with the superconductive phase in $x < 0$ and the substrate in $x > 0$. (○ Y^{3+}, □ Ba^{2+}, ● Cu^{2+}, ▲ Mg^{2+} in (a), Zr^{4+} in (b) and Al^{3+} in (c))

nominal ratio was located at a distance of about 37 μm, and for specimens sintered at 930 °C, the nominal ratio was located at a distance of about 3 μm.

3.2. Specimens with ZrO_2 substrates

The concentration profiles for specimens with ZrO_2 substrate sintered at 950 °C are shown in Fig. 3b. The diffusion path of Y^{3+} has a long tail in the substrate due to the yttrium additive in ZrO_2. The cation distributions in the film were nearly normal except for a small Y^{3+} peak. Unlike the case of MgO substrates, however, the concentration profiles were changed at higher sintering temperatures. In the 1000 °C specimens, uphill diffusion was common (Fig. 4). Concentration peaks were observed in all cation profiles (Y^{3+}, Ba^{2+}, and Cu^{2+}), and the Y^{3+} peak was over 40 wt %.

The penetration depth of Zr^{4+} in the superconductive film was about 15 μm in the 950 °C specimens. The distance did not change significantly in specimens sintered at 930 or 1000 °C. For specimens sintered at 900 °C, however, the penetration depth was decreased to about 5 μm and pores were found at the interface and in the interior of the film.

The nominal stoichiometric weight percentages of Y^{3+}, Ba^{2+}, and Cu^{2+} were measured at the distances of 35, 25, and 20 μm from the interface for specimens sintered at 1000, 950, and 930 °C, respectively. For specimens sintered at 900 °C, the presence of pores precluded making such a measurement.

3.3. Specimens with Al_2O_3 substrates

The diffusion characteristics of this group were denoted by the severe segregation of cations near the interface and a greater penetration depth of the Al^{3+} cations in the film region. Concentration profiles of a 950 °C specimen are shown in Fig. 3c which illustrate the general features. The details of the diffusion profiles have been reported elsewhere [22].

3.4. Comparison of results of 950 °C sintering

For comparison, the results of the three groups of specimens, all sintered at 950 °C for 1 h, are summarized. All three groups of specimens had good bonding, which was formed by cation interdiffusion. For the MgO substrate, the bonding was formed by diffusion of Y^{3+}, Ba^{2+}, and Cu^{2+} to the substrate.

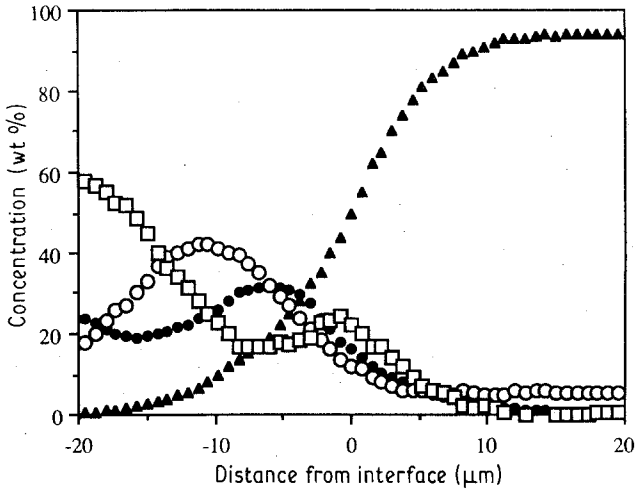

Figure 4 Cation distributions in an $YBa_2Cu_3O_{7-\delta}$–ZrO_2 couple. Specimen sintered at 1000 °C for 10 min. (○ Y^{3+}, □ Ba^{2+}, ● Cu^{2+}, ▲ Zr^{4+})

The amount of each cations transferred were proportional to its stoichiometric weight percentage and there was little effect on the overall stoichiometric ratio of the superconductive film. For the ZrO_2 substrate, the bonding-required interdiffusion occurred moderately from both sides, while with Al_2O_3 substrate, the bonding was due to diffusion of Al^{3+}. The bonding layer in a specimen with a MgO substrate is shown in Fig. 5. The holes were formed by ion bombardment during specimen preparation.

At 950 °C there was no significant segregation of cations in specimens with MgO or ZrO_2 substrate in contrast to the results of specimens with Al_2O_3. In the latter case, severe segregation of Cu^{2+} and Ba^{2+} was observed near the interface (Fig. 3c).

The penetration depths of the substrate cations, Al^{3+}, Mg^{2+}, and Zr^{4+}, in the film were different (Fig. 6). The large penetration depth of Al^{3+} (about 25 μm) and the severe segregation of Y^{3+}, Ba^{2+}, and Cu^{2+} in the film were likely to affect the superconducting behaviour of the oxide film. On the other hand, for films on a MgO substrate, the penetration depth of Mg^{2+} was very small (approximately 5 μm) and the Y^{3+}, Ba^{2+}, and Cu^{2+} cations were stoichiometrically

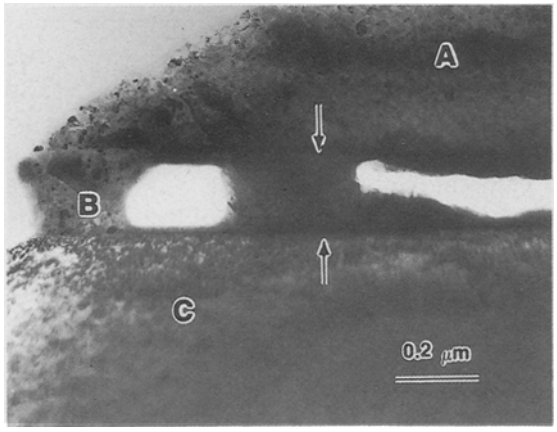

Figure 5 Bright field TEM image showing the bonding layer (B) formed in an $YBa_2Cu_3O_{7-\delta}$–MgO couple (A–C). Specimen sintered at 950 °C for 1 h.

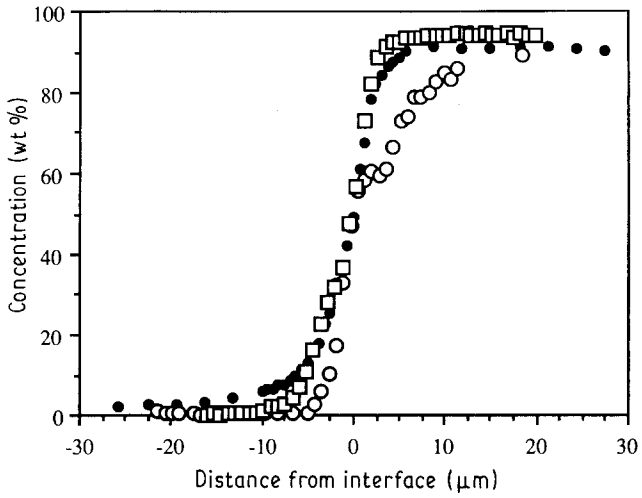

Figure 6 Penetration depths of substrate cations, Al^{3+}, Mg^{2+}, and Zr^{4+}. Specimens sintered at 950 °C for 1 h. (○ Mg^{2+}, □ Zr^{4+}, ● Al^{3+})

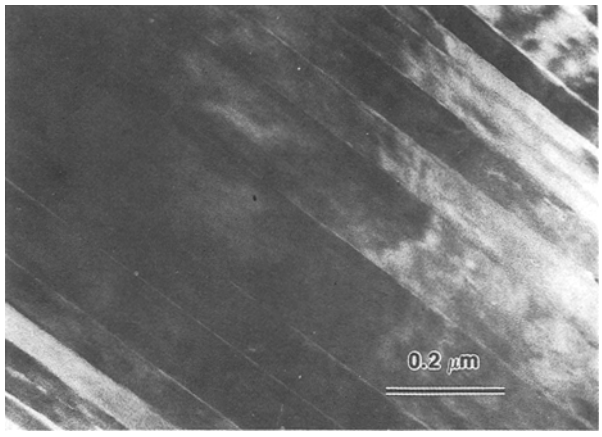

Figure 7 Bright field TEM micrograph showing twinned structure at 15 μm from the interface in a specimen of $YBa_2Cu_3O_{7-\delta}$ on MgO substrate. Specimen sintered at 950 °C for 1 h.

TABLE I Distance d from the interface to where the stoichiometric composition is resumed

Temperature (°C)	d (μm)			Bonding
	MgO	ZrO_2	Al_2O_3	
1000	37	35	> 40	good
950	15	25	40	good
930	3	20	—	poor

distributed close to the interface. These features seemed to ensure the superconductivity of the film, as shown in the resistance measurement (Fig. 1).

As mentioned earlier, the distance d from the interface to where the stoichiometric composition of the film was resumed varied for different substrates and sintering temperatures. For specimens sintered at 950 °C, the distances were 15, 25 and 40 μm for MgO, ZrO_2, and Al_2O_3 substrates, respectively. In the Al_2O_3 case, the distance was almost at the outer surface of the film. For reference, all d values measured for the three substrates sintered at 1000, 950, and 930 °C are given in Table I.

Micro-twins were observed in all the films examined [24–26]. A typical micrograph of a specimen sintered at 950 °C is shown in Fig. 7.

4. Conclusions

The interdiffusion between the $YBa_2Cu_3O_{7-\delta}$ oxide films and three substrates, Al_2O_3, MgO, and ZrO_2, was studied using analytical electron microscopy. Concentration profiles of Y^{3+}, Ba^{2+}, and Cu^{2+}, and Al^{3+}, Mg^{2+}, and Zr^{4+} were measured using characteristic X-rays. The results indicate that MgO and ZrO_2 are better substrate materials than Al_2O_3 and that a suitable sintering temperature is about 950 °C.

Acknowledgements

The authors are grateful to Dr D. M. Hiller and Dr J. I. Goldstein for technical discussions. XML and YTC acknowledge the financial support from the

Du Pont de Nemours and Company and from the Division of Materials Sciences, US Department of Energy under Grant DE-FG02-86ER45256.

References

1. M. K. WU, J. R. ASHBURN, C. J. TORNG, P. H. HOR, R. L. MENG, L. GAO, Z. J. HUANG, Y. Q. WANG and C. W. CHU, *Phys. Rev. Lett.* **58** (1987) 908, 911.
2. R. J. CAVA, B. BATLOGG, R. B. van DOVER, D. W. MURPHY, S. SUNSHINE, T. SIEGRIST, J. P. REMEIKA, E. A. RIETMAN, S. ZAHURAK and G. P. ESPINOSA, *ibid.* **58** (1987) 1676.
3. P. CHAUDHARI, R. H. KOCH, R. B. LAIBOWITZ, T. R. McGUIRE and R. J. GAMBINO, *ibid.* **58** (1987) 2684.
4. K. WATANABE, H. YAMANE, H. KUROSAWA, T. HIRAI, N. KOBAYASHI, H. IWASAKI, K. NOTO and Y. MUTO, *Appl. Phys. Lett.* **54** (1989) 575.
5. M. MURAKAMI, M. MORITA, K. DOI and K. MIYAMOTO, *Jpn J. Appl. Phys.* **28** (1989) 1189.
6. K. SALMA, V. SELVAMANICKAM, L. GAO and K. SUN, *Appl. Phys. Lett.* **54** (1989) 2352.
7. D. DIMOS, P. CHAUDHARI and J. MANNHANT, *Phys. Rev.* **B41** (1990) 4038.
8. S. JIN, T. H. TIEFEL, S. NAKAHARA, J. E. GRAEBNER, H. M. O'BRYAN, R. A. FASTNACHT and G. W. KAMMLOTT, *Appl. Phys. Lett.* **56** (1990) 1287.
9. M. R. NOTIS, M. OH, B. AVITZUR, Q. F. LIU and H. JAIN, in "Advances in Superconductivity", edited by Kitazawa and K. T. Ishiguro (Springer, New York, 1989) p. 371.
10. M. OH, Q. F. LIU, W. MISIOLEK, A. RODRIGUES, B. AVITZUR and M. R. NOTIS, *J. Amer. Ceram. Soc.* **72** (1989) 2142.
11. R. W. McCALLUM, J. D. VERHOEVEN, M. A. NOACK, E. D. GIBSON, F. C. LAABS and D. K. FINNEMORE, *Adv. Ceram. Mater.* **2** (1987) 388.
12. D. W. JOHNSON, Jr., E. M. GYORGY, W. W. RHODES, R. J. CAVA, L. C. FELDMAN and R. B. van DOVER, *ibid.* **2** (1987) 364.
13. M. ISHII, T. MAEDA, M. MATSUDA, M. TAKATA and T. YAMASHITA, *Jpn J. Appl. Phys.* **26** (1987) L1959.
14. J. P. SINGH, D. SHI and D. W. CAPONE, II, *Appl. Phys. Lett.* **53** (1988) 237.
15. K. TOGANO, H. KUMAKURA, H. SHIMIZU, N. IRISAWA and T. MORIMOTO, *Jpn J. Appl. Phys.* **27** (1988) L45.
16. R. C. BUDHANI, SING-MO H. TZENG, H. J. DOERR and R. F. BUNSHAH, *Appl. Phys. Lett.* **51** (1987) 1277.
17. I. SHIH and C. X. QIU, *ibid.* **52** (1988) 748.
18. H. KOINUMA, T. HASHIMOTO, M. KAWASAKI and K. FUEKI, *Jpn J. Appl. Phys.* **26** (1987) L399.
19. Y. H. HU and C. L. BOOTH, in "Advances in Superconductivity", *Superconductivity (ISS '88)* edited by Kitazawa and K. T. Ishiguro (Springer, New York, 1989) p. 647.
20. J. TABUCHI, A. OCHI, K. UTSUMI and M. YONEZAWA, *J. Ceram. Soc. Jpn* **96** (1988) 450.
21. J. TABUCHI and K. UTSUMI, *Appl. Phys. Lett.* **53** (1988) 606.
22. X. M. LI, Y. T. CHOU, Y. H. HU and C. L. BOOTH, *J. Mater. Sci. Lett.* **9** (1990) 669.
23. J. A. HEANLY and M. A. DAYANNANDA, *Met. Trans.* **17A** (1985) 983.
24. F. M. MUELLER, S. P. CHEN, M. L. PRUEITT, J. F. SMITH, J. L. SMITH and D. WOHLLEBEN, *Phys. Rev.* **B37** (1988) 5837.
25. R. K. SINGH, N. BIUNNO and J. NARAYAN, *J. Appl. Phys.* **65** (1989) 2398.
26. K. SASAKI, K. KURODA and H. SAKA, *Phil. Mag. Lett.* **59** (1989) 141.

Received 30 May
and accepted 26 June 1990